Available online at www.sciencedirect.com

ScienceDirect

Procedia Materials Science 3 (2014) 1226 – 1231

Procedia Materials Science

www.elsevier.com/locate/procedia

20th European Conference on Fracture (ECF20)

Critical stress for cleavage fracture in continuously cooled medium carbon V-microalloyed steel

Dragomir Glišić [a,*], Nenad Radović [a], Djordje Drobnjak [a], Abdunnaser Fadel [b]

[a] *Faculty of Technology and Metallurgy, University of Belgrade, Karnegijeva 4, 11120 Belgrade, SERBIA*
[b] *Al Zawiya University, Zawiya, LIBYA*

Abstract

Cleavage fracture of the medium carbon V-microalloyed steel with structure consisting of acicular ferrite, pearlite and grain boundary ferrite has been investigated by means of four-point bending of the notched samples at -196°C. It was found that cleavage fracture initiation has not been related to the coarse second phase particles cracking. Calculated values of the effective surface energy of 49 J/m^2 and critical cleavage fracture stress normalized by yield stress of 1.84 are in agreement with the results for the steels with ferrite-pearlite and bainite structures.

Selection and peer-review under responsibility of the Norwegian University of Science and Technology (NTNU), Department of Structural Engineering

Keywords: medium carbon V-microalloyed steel, acicular ferrite, critical fracture stress

1. Introduction

Medium carbon microalloyed steels have been developed in attempt to facilitate production of high strength steel products by direct cooling from the hot working temperature, thus to avoid complex and expensive procedure of quenching and tempering. Achieved satisfying high strength and fatigue resistance are accompanied by relatively poor impact toughness, in comparison with quenched and tempered steels. Certain improvement have been obtained in the steels with acicular ferrite structure, Linaza et al. (1993a), Ishikawa (1995). It is believed that high density of

* Corresponding author. Tel.: +381113303760; fax: +381113370387.
E-mail address: gile@tmf.bg.ac.rs

Selection and peer-review under responsibility of the Norwegian University of Science and Technology (NTNU), Department of Structural Engineering
doi:10.1016/j.mspro.2014.06.199

high-angle boundaries in fine interlocking structure of ferrite plates and laths provide an effective barriers for microcrack propagation, Linaza et al. (1993a), Linaza et al. (1996). Cleavage fracture of medium carbon microalloyed steels has been studied mostly for ferrite-pearlite and bainite structures, while the steels with predominantly acicular ferrite structure received relatively limited attention.

The aim of present work is to assess cleavage fracture mechanism in medium carbon V-microalloyed steel with predominantly acicular ferrite structure and to calculate local fracture stress.

2. Material and experiment

A commercial medium carbon V-microalloyed steel received as hot-rolled rods ∅19 mm, containing 0.256%C, 0.416%Si, 1.451%Mn, 0.0113%P, 0.0112%S, 0.201%Cr, 0.149%Ni, 0.023%Mo, 0.099%V, 0.002%Ti, 0.038%Al, 0.183%Cu, 0.002%Nb, 0.0229%N has been investigated. As-received microstructure was eliminated by homogenization treatment at 1250°C for 4 hours in argon protective atmosphere followed by oil quenching. Samples were afterwards austenitized at 1250°C for 30 minutes in argon and cooled at still air.

In order to investigate cleavage fracture of the steel, four-point bending (4PB) testing at liquid nitrogen temperature (-196°C) was performed with constant crosshead speed of 0.1 mm/min. Griffiths-Owen type of four point bending specimens with round notch were used, Griffiths and Owen (1971).

Finite element modeling (FEM) was used to calculate stress and strain distributions along the distance from the notch root in 4PB specimen at the instant of fracture. Finite element calculations were performed using ABAQUS software. Half of the specimen was modeled in two dimensions, assuming plain strain conditions. Quadratic eight-node plane strain full integration elements were used (CPEG8). Mesh was most refined along the notch root, with minimal element size of $2 \cdot 10^{-3}$ mm. Largest element size was 2 mm. Total number of elements was 21746. Mechanical properties of the steel were modeled by true stress-true strain curves; Young's modulus of 200 GPa and Poisson's ratio of 0.28 were used.

Tensile testing was performed at liquid nitrogen temperature at constant crosshead speed of 0.1 mm/min. Cylindrical specimens 6 mm in diameter and with 30 mm gauge length were used. Experimental true stress-true strain data were modeled by polynomial regression analysis.

Scanning electron microscope (SEM) equipped with energy dispersive X-ray spectrometer (EDS) was used for fracture surface analysis. Cleavage fracture origin was found by tracing back markings at the fracture surface. Distance of the cleavage initiation site from the notch root, X_0, and dimensions of the first cleavage facet were measured from the SEM micrographs.

Local fracture stress, σ_F^*, was determined from the distribution of maximum principal stress calculated by FEM at the distance of the cleavage initiation site from the notch root, X_0. Critical fracture stress, σ_F^*, and diameter of the critical circular microcrack, D, are related by Griffith's equation, Echeverria et al. (2003), Curry and Knott (1978):

$$\sigma_F^* = \sqrt{\frac{\pi \cdot E \cdot \gamma}{\left(1-\nu^2\right) \cdot D}} \tag{1}$$

where γ is the effective surface energy, E is the modulus of elasticity and ν is the Poisson's coefficient. Microcrack diameter D was approximated by effective diameter of the first cleavage facet D_{eff}, Echeverria et al. (2003), Alexander and Bernstein (1989):

$$D_{eff} = \frac{D_{\min}}{\phi^2}\frac{\pi^2}{4}, \quad \phi = \frac{3\pi}{8} + \frac{\pi}{8}\left(\frac{D_{\min}}{D_{\max}}\right) \tag{2}$$

where D_{max} and D_{min} represent maximum and minimum ferret diameter of the first cleavage facet.

3. Results and Discussion

Microstructure of the V-microalloyed steel air cooled from 1250°C (Fig. 1) consists of acicular ferrite (AF), pearlite (P) and grain boundary ferrite (GBF). Acicular ferrite is predominant microconstituent, occupying the most of the previous austenite grain interiors. Previous austenite grain boundaries are decorated by thin network of proeutectoid ferrite grains, most of which are polygonal idiomorphs. Elongated alotriomorphic ferrite grains could be found also. One example alongside with Widmanstätten saw-teeth (WST) ferrite plates emanating from grain boundary alotriomorph is pointed out on micrograph in Fig. 1a. Grain boundary ferrite is separated from acicular ferrite by layer of very fine pearlite. High volume fraction of acicular ferrite, as a product of displacive transformation of austenite, indicates relatively high hardenability of the steel. It could be ascribed to the effect of alloying with manganese, well known for strong retarding effect on diffusive transformations of austenite, alongside with chromium, nickel and molybdenum, Krauss (2005), Bhadeshia (2006). However, proeutectoid ferrite nucleation at austenite grain boundaries has not been suppressed. Excess carbon from the ferrite enriches neighboring austenite, stabilizes it and consequently delays its transformation to lower temperatures, where diffusion becomes sluggish, and as a result displacive transformation is taking place. Considering that proeutectoid ferrite precludes nucleation of bainite at grain boundaries, intragranular nucleation of acicular ferrite is promoted, Bhadeshia (2001). Moreover, VN particles are the most potent sites for heterogeneous nucleation of acicular ferrite, Ishikawa (1995), Garcia-Mateo (2008a), Garcia-Mateo (2008b). In the case of a V-microalloyed steel with high nitrogen content, abundant precipitation of VN particles is expected, especially in the presence of MnS inclusions as suitable VN nucleation sites, Furuhara (2003).

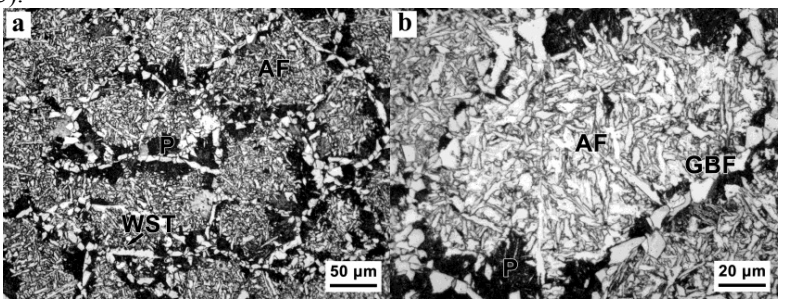

Fig. 1. (a) Acicular ferrite with pearlite and network of grain boundary ferrites; (b) acicular ferrite needle-like structure.

Fracture surface exhibits typical transgranular cleavage fracture (Fig. 2). Most of the facets have irregular shape with curved edges, giving fracture surface feathery look. Propagating cracks interconnect leaving sharp, curved edges, which appear brighter due to SEM image “edge effect”. Small irregular facets reflect the appearance of the acicular ferrite structure, while coarser facets resemble fractured ferrite and pearlite grains or their agglomerates with the similar crystallographic orientation. Chevron-like trace on the fracture surface point to the area of cleavage origin, while very fine river lines at cleavage facets lead back to the fracture initiation site (Fig. 2a). Typical example of river lines that could be traced back to the cleavage origin is shown in Fig. 2b.

Fracture origin is placed very close to the notch root, practically at the border with stretch zone of the 4PB specimen. No broken second phase particles at the initiation site were found. Moreover, no distinct microstructural feature responsible for cleavage initiation could be found in none of the 4PB specimens. Cleavage initiation in microalloyed steels with ferrite-pearlite or bainitic structures is in most cases related to the fracture of coarse brittle particles, such as TiN or MnS, Linaza et al. (1993b), Linaza et al. (1995), Echeverria and Rodriguez-Ibabe (2004). On the other, similarly to results in this work, a cleavage initiation near the notch root not related to the broken second phase particles in predominantly acicular ferrite structure had been reported earlier by Echeverria and Rodriguez-Ibabe (2003).

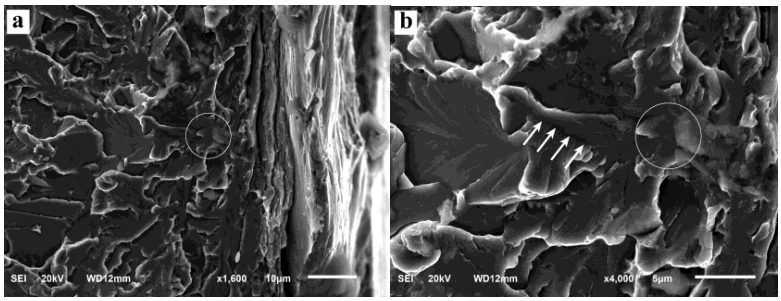

Fig. 2. (a) Cleavage origin in a 4PB specimen; (b) Cleavage initiation site and high-angle boundary passed by the microcrack.

A different model for cleavage initiation, by fracture of grain boundary carbides, should be considered here. Mechanism proposed by Smith, as a modified Cottrell's mechanism of fracture initiation, implies that stress field developed in front of dislocation pile-ups causes fracture of elongated carbides at ferrite grain boundaries, Ghosh et al. (2013). Those elongated carbides with longer axis oriented in the direction of applied tensile stress, additionally forced to elongate with ductile ferrite matrix, consequently easily break. Newly formed microcracks continue propagation through ferrite grains, Smith (1968), Fairchild et al. (2000). Obviously, this mechanism implicates the role of plastic deformation in cleavage fracture initiation. As it had been elaborated in previous investigations, in addition to critical fracture stress value, a critical plastic strain for cleavage fracture had been suggested, Chen et al. (2002), Chen et al. (2003), Yu et al. (2006). In this way, it could be argued that cleavage origin is placed so close to the notch root where plastic strain is highest. Microcrack propagates further through the matrix at the instant when local stress attains critical level. Cleavage fracture is a three-step process, which includes microcrack nucleation, propagation through the particle/matrix interface and finally propagation through the high angle boundaries of the matrix, Knott (1992). Additionally, this process must develop in a dynamic way, meaning that interruption would cause sharp cleavage crack to blunt. In case of Smith's mechanism, first two steps are actually combined within the process of grain boundary carbides fracture and propagation of the microcrack through the ferrite grain. It has been confirmed that microcracks formed in ferrite would grow uninterruptedly up to the high angle boundary Ghosh et al. (2013). Moreover, there are reports of relatively easy propagation of microcracks through ferrite-pearlite units of the same crystallographic orientation, thus forming large initial cleavage microcracks, San Martin and Rodriguez-Ibabe (1999).

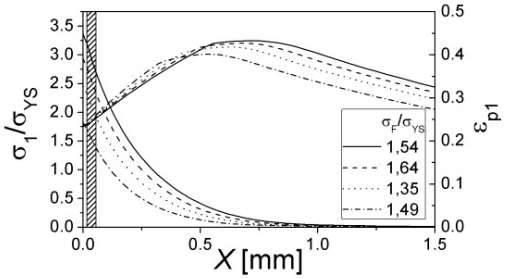

Fig. 3. Maximum principal stress and plastic strain along the distance from the notch root of the 4PB specimen.

Distributions of the maximum principal stress and plastic strain along the distance from the notch root, for all tested 4PB specimens, are shown in Fig. 3. It is clear that cleavage fracture originates from the zone of high plastic strain, highlighted by shaded area at the diagram. Distance from the notch root and dimensions of the first cleavage facets for all specimens are given in Table 1, alongside with results of 4PB test and FEM calculations. Although values of maximum bending load, F_{max}, macroscopic fracture stress, σ_F, and critical plastic strain, ε_{pc}, exhibit considerable variations, local fracture stress, σ_F^*, normalized by yield stress, remains in relatively narrow range between 1.78 and 1.92. Average value of critical fracture stress, σ_F^*, is 1416.4 MPa.

Table 1. Results of 4PB test, FEM calculations and fractographic measurements.

	F_{max} [N]	σ_F [MPa]	σ_F/σ_{YS}	X_0 [μm]	$\sigma_F^*=\sigma_1(X_0)$ [MPa]	σ_F^*/σ_{YS}	ε_{pc}	$D_{max}\times D_{min}$ [μm]	D_{eff} [μm]
1	28521.6	1192.7	1.54	29.2	1412.9	1.82	0.350	51.7×23.8	34.70
2	30318.1	1267.8	1.64	16.7	1380.2	1.78	0.424	29.3×14.2	21.71
3	25084.6	1049.0	1.35	19.4	1400.6	1.81	0.219	19.2×16.0	18.76
4	27561.2	1152.5	1.49	47.4	1471.9	1.90	0.266	29.7×14.0	21.57
AVG	**27871.4**	**1165.5**	**1.505**	**28.175**	**1416.4**	**1.8275**	**0.31475**		**24.18**

Critical cleavage fracture stress analysis was performed under the assumption that first cleavage facet correspond to the initial microcrack, whose size is greater than or equal to the critical size under the applied stress, in accordance with Griffith's equation (1). Therefore, effective surface energy, γ, for cleavage crack propagation through the matrix was calculated from the $\sigma_F^*–D_{eff}^{-1/2}$ plot, shown in Fig. 4a. Considering that first cleavage facet corresponds to one ferrite grain or one "ferrite unit", it could be assumed that the value of effective surface energy should be determined from the line drawn below all data points in the diagram, thus representing an upper bound value. In that way, a value for effective surface energy of 49 J/m^2 has been calculated. It is in good agreement with value of 50 J/m^2 calculated in earlier studies of cleavage fracture in medium carbon microalloyed steels, San Martin and Rodriguez-Ibabe (1999), Linaza et al. (1997), Rodriguez-Ibabe (1998). Previous results, mostly for ferrite-pearlite medium carbon steels, are summarized alongside with present measurements on $\sigma_F^*–D_{eff}^{-1/2}$ plot in Fig. 4b.

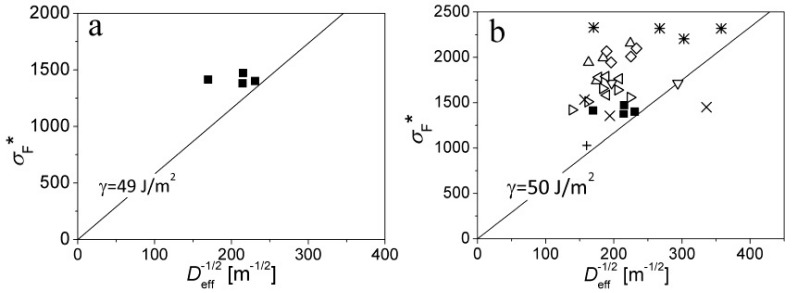

Fig. 4. (a) Values of the local critical fracture stress plotted against first cleavage facet effective diameter; (b) comparison with measurements from the literature, Linaza et al. (1997), Rodriguez-Ibabe (1998).

Large variation in ε_{pc} implies that it should not be taken as a critical condition for cleavage fracture, as it had been suggested by Chen et al. (2002), Chen et al. (2003), Yu et al. (2006). It could be assumed that it is rather critical size of microcracks in the field of stress in front of the notch root. According to the Smith's mechanism, microcrack diameter depends on ferrite grain (or "ferrite unit") size. The role of microstructure and actual deformation mechanism in the plastic zone in front of the notch root should be considered. In present case of dominantly acicular ferrite structure with considerable volume fraction of grain boundary ferrite with adjacent pearlite nodules/colonies, Smith's mechanism of cleavage fracture could be proposed. Nevertheless, a value of effective surface energy is approximately the same as for other medium carbon microalloyed steels where different initial microcrack nucleation mechanisms had been observed. Fine-grained acicular ferrite structure has not exerted any effect on critical fracture stress or effective surface energy at -196°C, in the presence of pearlite and eutectoid ferrite.

4. Conclusions

Cleavage fracture of the medium carbon V-microalloyed steel with predominantly acicular ferrite structure, alongside with pearlite and proeutectoid ferrite, was initiated by grain boundary carbides fracture in the zone of high plastic strains ahead of the notch root of the 4PB specimen. As microcrack is nucleated at grain boundary carbides within ferrite-pearlite unit, it readily propagates up to the high angle boundary and further throughout the matrix. Average critical fracture stress and effective surface energy has been calculated to be 1416.4 MPa and 49 J/m2,

respectively, which is in agreement with values determined for microalloyed medium carbon steels with ferrite-pearlite or bainite structures found in the literature.

Acknowledgements

The authors are indebted to Ministry of Education and Science of Serbia for financial support (Project OI174004) and Serbian Oil Company for supplying experimental material.

References

Linaza, M.A., Romero, J.L., Rodriguez-Ibabe, J.M., Urcola, J.J., 1993. Improvement of fracture toughness of forging steels microalloyed with titanium by accelerated cooling after hot working. Scripta Metallurgica et Materialia 29, 1217-1222.

Ishikawa, F., Takahashi, T., 1995. The Formation of Intragranular Ferrite Plates in Medium-carbon Steels for Hot-forging and Its Effect on the Toughness. ISIJ International 35, 28–33.

Linaza, M.A., Romero, J.L., San Martín, I., Rodriguez-Ibabe, J.M., Urcola, J.J., 1996. Improvement of Toughness by Stopping Brittle Process Nucleated in Ceramic Particles Through Thermomechanically Optimized Microstructures in Engineering Steels, in: "*Microalloyed Bar and Forging Steels*", C.J. Van Tyne, G. Krauss, D.K. Matlock (Eds.). TMS, Golden, Colorado, 1996, pp.311.

Griffiths, J.R., Owen, D.R., 1971. An Elastic-Plastic Stress Analysis for a Notched Bar in Plane Strain Bending, Journal of the Mechanics and Physics of Solids 19, 419–431.

Echeverria, A., Rodriguez-Ibabe, J.M., 2003. The role of grain size in brittle particle induced fracture of steels. Materials Science and Engineering: A 346, 49–158.

Curry, D.A., Knott, J.F., 1978. Effect of microstructure on cleavage fracture stress in steel. Metal Science 12, 511-514.

Alexander, D.J., Bernstein, I.M., 1989. Cleavage fracture in pearlitic eutectoid steel. Metallurgical Transactions A 20, 2321-2335.

G. Krauss, 2005. Steels: Processing, Structure, and Performance, ASM International.

Bhadeshia, H.K.D.H., Honeycombe, R. 2006. Steels: Microstructure and Properties, 3rd ed., Elsevier.

Bhadeshia, H.K.D.H., 2001. Bainite in Steels: Transformations, Microstructure and Properties, 2nd ed., IOM Communications Ltd., London.

Garcia-Mateo, C., Capdevila, C., Caballero, F.G., De Andrés, C.G., 2008. Influence of V Precipitates on Acicular Ferrite Transformation Part 1: The Role of Nitrogen. ISIJ International, 48, 1270–1275.

Garcia-mateo, C., Cornide, J., Capdevila, C., Caballero, De Andrés, C.G., 2008. Influence of V Precipitates on Acicular Ferrite Transformation Part 2: Transformation Kinetics. ISIJ International, 48, 1276–1279.

Furuhara, T., Shinyoshi, T., Miyamoto, G., Yamaguchi, J., Sugita, N., Kimura, N., 2003. Multiphase Crystallography in the Nucleation of Intragranular Ferrite on MnS-V(C,N) Complex Precipitate in Austenite. ISIJ International, 43, 2028–2037.

Linaza, M.A., Romero, J.L., Rodriguez-Ibabe, J.M., Urcola, J.J., 1993. Influence of the microstructure on the fracture toughness and fracture mechanisms of forging steels microalloyed with titanium with ferrite-pearlite structures. Scripta Metallurgica et Materialia 29, 451-456.

Linaza, M.A., Romero, J.L., Rodriguez-Ibabe, J.M., Urcola, J.J., 1995. Cleavage fracture of microalloyed forging steels. Scripta Metallurgica et Materialia 32. 395-400.

Echeverria, A., Rodriguez-Ibabe, J.M., 2004. Cleavage micromechanisms on microalloyed steels. Evolution with temperature of some critical parameters. Scripta Materialia 50, 307–312.

Ghosh, A., Ray, A., Chakrabarti, D., Davis, C.L., 2013. Cleavage Initiation in Steel: Competition between Large Grains and Large Particles. Materials Science and Engineering: A 561, 126–135.

Smith, E., 1968. Cleavage Fracture in Mild Steel. International Journal of Fracture Mechanics 4, 131-145.

Fairchild, D.P., Howden, D.G., Clark, W.A.T., 2000. The mechanism of brittle fracture in a microalloyed steel: Part II . Mechanistic Modeling, Metallurgical and Materials Transactions 31A, 653–667.

Chen, J.H., Wang, G.Z., Wang, Q., 2002. Change of Critical Events of Cleavage Fracture with Variation of Microscopic Features of Low-Alloy Steels. Metallurgical and Materials Transactions 33A, 3393–3402.

Chen, J.H., Wang, Q., Wang, G.Z., Li, Z., 2003. Fracture behavior at crack tip - a new framework for cleavage mechanism of steel. Acta Materialia 51, 1841–1855.

Yu, S.R., Yan, Z.G., Cao, R., Chen, J.H., 2006. On the change of fracture mechanism with test temperature. Engineering Fracture Mechanics 73, 331–347.

Knott, J.F., 1992. Micromechanisms of fracture: The role of microstructure, Reliability and Structural Integrity of Advanced Materials, ECF9, S. Sedmak, A. Sedmak, D. Ruzic, Eds., EMAS, pp.1375.

San Martin, J.I., Rodriguez-Ibabe, J.M., 1999. Determination of energetic parameters controlling cleavage fracture in a Ti-V microalloyed ferrite-pearlite steel. Scripta Materialia 40, 459–464.

Linaza, M.A., Rodriguez-Ibabe, J.M., Urcola, J.J., 1997. Determination of the energetic parameters controlling cleavage fracture initiation in steels. Fatigue & Fracture Engineering Materials & Structure 20, 619–632.

Rodriguez-Ibabe, J.M., 1998. The Role of Microstructure in Toughness Behaviour of Microalloyed Steels, Materials Science Forum 284-286, 51-62.